Advances in Science and Technology Research Journal

Advances in Science and Technology Research Journal, 2026, 20(9), 302–313
https://doi.org/10.12913/22998624/224425
ISSN 2299-8624, License CC-BY 4.0

Received: 2026.05.20
Accepted: 2026.07.10
Published: 2026.08.01

Study of geometric morphology control in generalized α, λ, s Bezier curves based on statistical analysis

Rasha Jabbar[1*], Samah A. Aufy[1], Waad Q. Shiaa[1]

[1] Department of Industrial and Systems Engineering, College of Production Engineering and Metallurgy, University of Technology, Baghdad, Iraq

* Corresponding author's e-mail: rasha.j.alasadi@uotechnology.edu.iq

ABSTRACT

The main objective of Computer Aided Geometric Design (CAGD) is the construction of a high-quality Bezier curve that satisfies design requirements and ensures high manufacturing efficiency. This research aimed to investigate the behavior of the Bezier curve with shape parameters (α, λ, s) resulting in Generalized Bezier curves. The main goal was to yield minimum surface area from the Generalized Bezier surface of revolution to enhance manufacturing efficiency, material usage, and fabrication. To study the influence of shape parameters on curve geometric morphology, it is required to generate a miscellaneous design with a range of shape parameter values and then statistically evaluate. Also, the Taguchi method was used to investigate the most significant contribution of each parameter that yields the minimum surface area. ANOVA results indicated that parameters S & λ have the most significant influence on the SA. The results clarified the non-linear behavior between shape parameters that makes the direct prediction of curve configuration intricate for variations of shape parameters, especially for S-curve shapes.

Keywords: Bezier curve, shape parameters, Bezier Bernstein polynomials, α, λ, s parameters, Taguchi, ANOVA

INTRODUCTION

Curves and surfaces are very important for the design of geometrical shapes, and is used extensively in many applications, such as the automotive, shipbuilding, and aerospace industries, architectural design, and computer animation, technological and geometric design using CAD system [1]. A popular way of modeling geometry in CAD is to represent the outer surface, or curve, of the object as a patchwork of parametric polynomial pieces. Bezier curves and surfaces are an effective representation of such polynomial pieces that makes their interactive design easier and more intuitive than with other representations. They were developed in the 1960s and 1970s by Paul de Casteljau and Pierre Bezier, for use in the automotive industry [2].

One challenge in using a classical Bezier curve is the limited ability to vary or adjust its shape without altering the control points. Therefore, researchers have started reconstructing the representation of Bezier curve, such as rational curves [3], trigonometric curves [4], a cubic spiral Bezier curve [5], Bezier-like curves [6], and Bezier curve with shape parameters [2], and many other Bezier curve modifications.

Shape parameters provide a flexible influence on geometric morphology within the investigated parameter range. These geometric variations directly influence the surface area of the structure [7]. This highlights the importance of minimizing SA as a design objective. In additive manufacturing, lower SA is associated with reduced geometric complexity, fewer layer transitions, leading to improved printability and manufacturing efficiency. Therefore, Bezier-based modeling provides an effective, flexible geometric mechanism using parameter values that minimize SA [8].

This study systematically investigated the effects of shape parameters (α, λ, s) values in Bezier curves and determined the most effective parameter on SA.

BACKGROUND

Historically, Farouki (2012) stated the history of the Bernstein basis functions of the Bezier curve and highlighted its advantages [9]. However, these curves are limited in representing transcendental curves due to the polynomial form of the Bernstein operator. Another limitation is the dependency of the curve shape on the control points. To address these limitations, recent advancement in the field of Bezier curve and surface enhanced the generation of flexible Bezier curve. Farin et al. (2002) defined the rational Bezier curve as an extended classical Bezier curve by introducing weights for each control point, providing greater flexibility in curve geometric morphology without changing the control points [1]. Although rational Bezier curve provides greater flexibility through the use of weights, defining the appropriate weights values is often non- intuitive and may lead to undesirable shape distortions [3]. To overcome these limitations, several researchers introduced shape parameters into Bernstein basis functions. These parameters allow designers to modify the curve geometry without changing the control points.

Wang and Wang (2005) used an integral method with shape parameters to approximate the control polygon, though geometric interpolation remained difficult [10]. Yang and Zeng (2009) investigated Bezier curves and surfaces through various values of shape parameter modification intuitively, foreseeably, and precisely [11]. Also, Chen (2013) introduced Quasi-Bezier curves based on a Quasi-Bernstein basis, enabling flexible shape manipulation via parameters without changing control points, offering superior geometric flexible mechanism [12].

In addition, Zhu and Han (2015) [13], Bashir and Jamaludin (2016) [14], Wu et al. (2014)[15], Hu et al. (2014) [16], Nazir et al. (2016) [17], and Li et al. (2018) [18] proposed Bezier curves with multiple local shape parameters, which make the local shapes of the curves and surfaces can be modified conveniently without altering the control vertices. Then, Maqsood et al. (2020) introduced generalized blended trigonometric Bezier curves with two shape parameters, offering superior shape adjustability and precision for modeling complex, free-form engineering shapes compared to classical methods [19]. Gezer et al. (2022) introduced a novel family of λ and α operators offering superior convergence behaviors and preserving essential shape characteristics such as monotonicity and convexity [20]. Lu and Guicang (2022) introduced a new class of Bezier curves and surfaces with three shape parameters, offering enhanced flexibility for complex surface modeling and design [21]. Zhang and Wang (2025) introduced α-sh basis functions to construct curves and surfaces with adjustable shape parameters [22]. Zhou and Cai (2025) introduced generalized blending-type Bernstein operators and (λ, μ) parameters that allow better error control, making them ideal for high-accuracy tasks like medical imaging and CNC machining paths [23]. Canlı and Şenyurt (2025) introduces hybrid α-sh basis functions that allow for precise local tension control and shape in aerospace as well as lens design without altering the overall structure [24].

CONSTRUCTION OF BEZIER BASIS WITH SHAPE PARAMETER

The classical Bezier curves are wildly utilized in CAGD defined by Bernstein polynomials with nth degree, Bernstein polynomials are defined as in Equation 1 [2]:

$$U_{k,n}(t) = \frac{n!}{k!\,(n-k)!}\, t^{k}(1-t)^{n-k} \quad (1)$$

For s = 0, 1, 2, …. n, $\frac{n!}{k!\,(n-k)!}$ are binomial coefficient, usually, $U_{k,n}(t)=0$ if k<0 or k>n.

Suppose P0, P1,. Pn be (n+1) the given control points, then Bezier curve is defined as in Equation 2 [2]:

$$p_{k,n}(t) = \sum_{k=0}^{n} U_{k,n}(t)P_k \quad 0 \le t \le 1 \quad (2)$$

where: $U_{k,n}(t)$ the Bernstein polynomials give in Equation 1.

In [25], α-Bezier curves with α shape parameter are constructed as in Equation 3:

$$p_{k,n}^{\alpha}(t) = \sum_{k=0}^{n} U_{k,n}^{\alpha}(t)\, P_k \quad 0 \le t \le 1 \quad (3)$$

where: for α Î(0,1), $U_{k,n}^{\alpha}$ are α- Bernstein polynomials that were introduced in [26] as in Equation 4:

$$U_{k,n}^{\alpha}(t) = \begin{bmatrix} \binom{k-2}{s}(1-\alpha)t + \binom{k-2}{n-2} \\ (1-\alpha)(1-t) + \binom{k}{n}\alpha t(1-t) \end{bmatrix} \quad (4)$$

$$t^{n-1}(1-t)^{k-n-1}$$

Ye et al. [27] introduced and studied new Bezier basis with a shape parameter λ ∈ (–1, 1), which is defined by Equation 5

$$U(t)^{\lambda}_{k,n} = \begin{cases} U_{0,n}(t) - \dfrac{\lambda}{n+1} U_{1,n+1}(t), \\ if\ k = 0 \\ U_{k,n}(t) + \lambda\left(\dfrac{n-2k+1}{n^2-1} U_{k,n+1}(t)\right) - \\ -\lambda\left(\dfrac{n-2k+1}{n^2-1} U_{k+1,n+1}(t)\right) \\ if\ (1 \le k \le n-1) \\ U_{n,n}(t) - \dfrac{\lambda}{n+1} U_{n+1,n}(t)\ if\ k = n \end{cases} \tag{5}$$

By combining λ- and α- Bernstein polynomials stated in [19] with the positive parameter s, (λ, α, s) Bernstein polynomials can be defined as in Equation 6 [28, 29]:

$$U(t)^{\lambda,\alpha,s}_{k,n} = \begin{cases} U(t)^{\lambda}_{k,n}\ if\ n < s \\ (1-\alpha)\begin{bmatrix} tU(t)^{\lambda}_{k-s,n-s} + \\ +(1-\alpha)U(t)^{\lambda}_{k,n-s} \end{bmatrix} \end{cases} \tag{6}$$

$$+\ \alpha U(t)^{\lambda}_{k,n}\ if\ r \ge s$$

for t, α ∈ (0,1), λ ∈ (-1,1), and s is any positive integer note. The (λ, α, s) Bernstein polynomial basis reduced to the classical Bernstein polynomial basis when λ = 0, α = 1, and s = 1.

$U(t)^{\lambda,\alpha,s}_{k,n}$ is non-negative.

End point polarization:

$$U(0)^{\lambda,\alpha,s}_{k,n} = \begin{cases} 0, k \ne 0 \\ 0, k = 0 \end{cases}, U(1)^{\lambda,\alpha,s}_{k,n} \begin{cases} 0, k \ne n \\ 1, k = n \end{cases},$$

Symmetry:

$$U(t)^{\lambda,\alpha,s}_{k,n} = U(1-t)^{\lambda,\alpha,s}_{k,n}$$

Partitioning of unity:

$$\sum_{k=0}^{n} U(t)^{\lambda,\alpha,s}_{k,n} = 1$$

Figure 1 shows the fifth-order generalized Bernstein basis functions for different values of (α, λ, s) parameters compared to the classical Bernstein basis functions.

In Figure 2 the geometric properties are satisfied by the (λ, α, s)-Bezier curves with different shape parameter values. By changing the values of one parameter, the shape of the curve is adjusted without changing the control points, preserving the geometry of classical Bezier curves.

IMPLEMENTATION OF THE STUDY

The use of shape parameters is essential to enhance the flexibility of Bezier curve representations beyond the limitations of control points alone. While control points define the general outline of the curve, they do not provide sufficient capability to finely regulate the curvature distribution along the profile. By introducing shape parameters, additional degrees of freedom are incorporated, allowing systematic and continuous variation of the curve shape without altering its structural formulation. This parametric control enables the generation of a wide

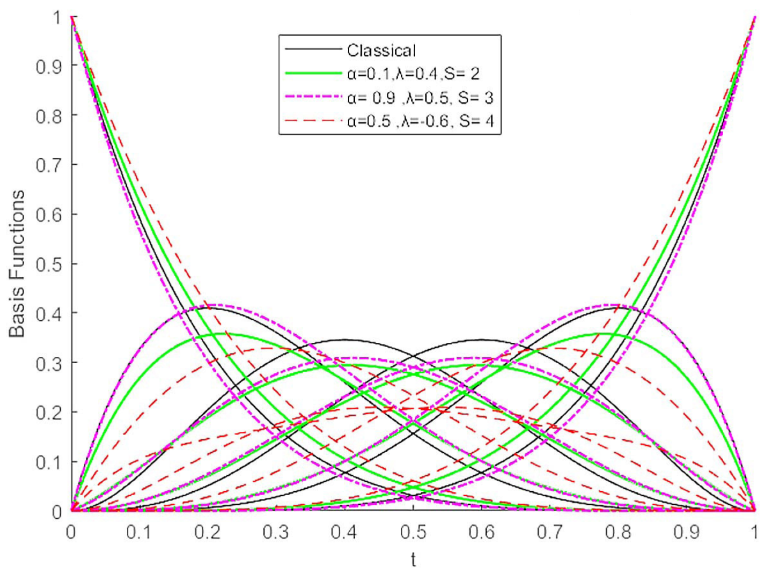

Figure 1. Classical and (λ, α, s) Bezier Bernstein polynomials

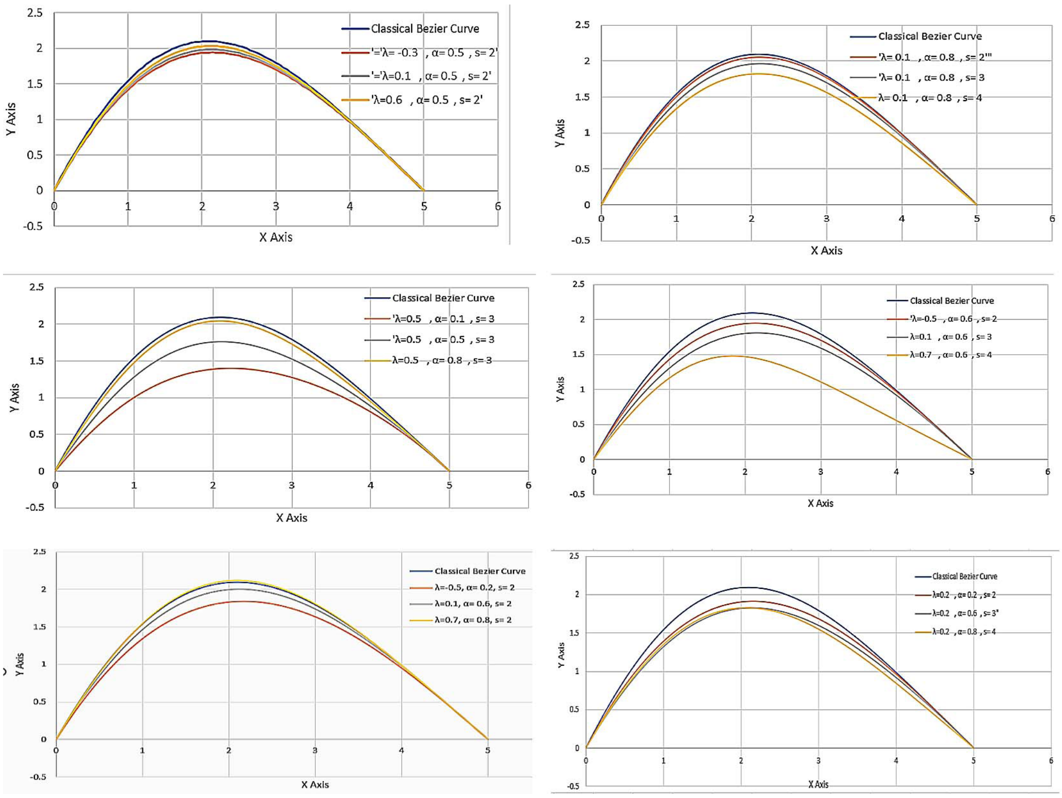

Figure 2. (α, λ, s)-Bezier curves with multiple values of shape parameters vs. classical Bernstein curves

range of geometries from a single mathematical model, making it particularly suitable for design exploration.

In the context of this study, (λ, α, s) shape parameters are utilized to produce different curve profiles that, upon revolution, result in diverse three-dimensional surfaces with various surface areas. The goal is the geometry that meets the minimum surface area to enhance part fabrication. This variation is critical for investigating the influence of geometry on the surface area. To clarify this goal, a Bezier curve of the 5th degree defined by the control points (p0, p1, ..., p5) is adopted with different values of shape parameters (λ, α, s) that generate miscellaneous 2d S-curve shapes, as shown in Figure 3.

In order to visualize and understand the individual influence of each shape parameter on Bezier curve behavior and the generated surface area, a series of geometrical experiments was conducted. More than 45 experimental configurations were generated. The generated curve shapes demonstrated a geometric interpretation of how the parameters affect the curvature, smoothness, and surface area. Keeping in mind that the intended surface is generated by revolving the Bezier curve around the y-axis. The revolved surface generated by revolving the classical Bezier curve defined by control points is shown in Figure 4 with a surface area equal to 64129.9 mm^2.

The effect of each parameter on the part surface area is analyzed by altering one parameter while keeping the other constant and calculating the surface area. As the limits of the shape parameters are $\lambda \in (-1, 1)$, $\alpha \in (0, 1)$, $S \in (2, 4)$, the results of 45 experiments demonstrated a flexible influence on geometric morphology introduced by shape parameters. when s = 2, 3, and 4. The results when s = 2 are illustrated in Table 1 and Figure 5. It depicts the revolved surfaces of the generalized Bezier cures for the 25 experiments when S equal to 2.

When s=2, the geometric experiments shows that the generalized Bezier curve preserved the S-curve shape and nearly close to the classical Bezier configuration with only a little trend in curvature and surface area under different combinations of shape parameter.

As depicted in Figure 6, the interaction plots between the shape parameters when s=2 and the classical Bezier curve demonstrated the stable and weak interaction between λ and α. As well as the influence of one parameter constantly independent of the other, when λ = 0.6 and α= 0.8, the surface area exceeds the classical Bezier curve.

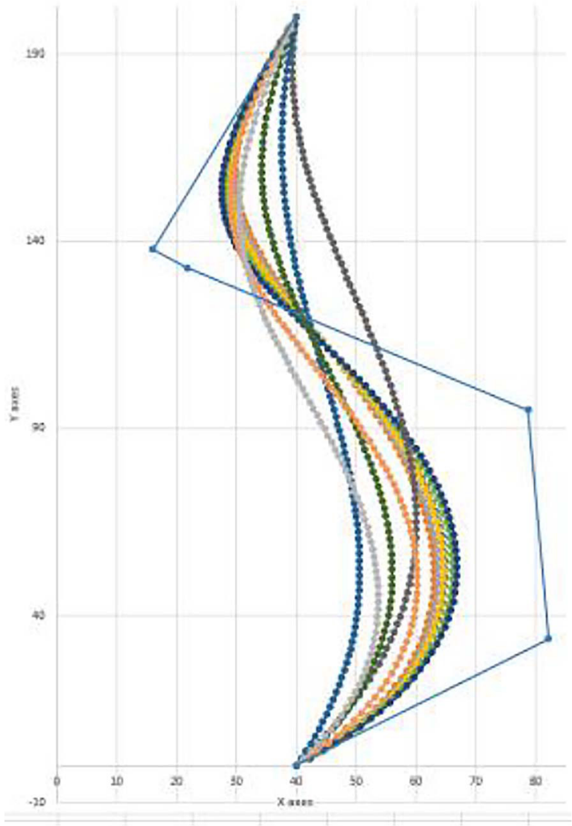

Figure 3. Curve construction with different (λ, α, s) values

The results of experiments when S=3 is depicted in Table 2 and Figure 7. It depicts the revolved surfaces of the generalized Bezier curves for the 25 experiments when s =3.

The geometric experiments reveals that when s=3, the generalized Bezier curve greatly deviates from the S-curve shape to a nearly cylindrical configuration when α = 0.1, regardless of the λ value. The effect starts to reduce slightly when the value of α increases, and the inflection zone was made explicit gradually when λ value increased.

When s=3, the interaction plots between the shape parameters classical Bezier curve signifies construing. It is clear that the value of α increasingly depend on the value of λ. The increasing divergence between the curves at higher values of α indicates a nonlinear interaction between the shape parameters. the surface area of all combinations is less than the classical Bezier curve, as shown in Figure 8.

The results of experiments when s=4 is depicted in Table 3 and Figure 9.

The generalized Bezier curve at s=4 demonstrated entirely different morphological behavior of the S-shape and the surface area when α =0.1. As the value of λ is negative, the surface configuration tends to be overblown, whereas the positive values introduce thinning geometry, grading to an obvious inflection zone. Also, smaller values of α generate an aggressive shape deformation that decreases gradually at larger

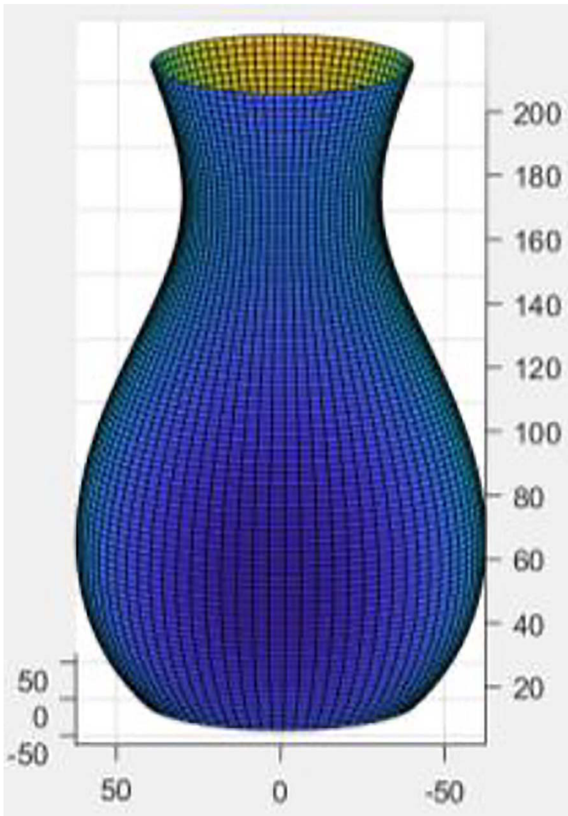

Figure 4. Classical Bezier revolves surface

Table 1. Results of 25 experiments when S=2, TFC – trend from the classical

λ	α1 = 0.1↓90%	TFC	α2 = 0.5↓50%	TFC	α3 = 0.8↓20%	TFC
λ1 = -0.9↓90%	59518.08	↓ 7%	60875.48	↓ 5%	62011.03	↓ 3.3%
λ2 = -0.5↓50%	59928.36	↓ 6.5%	61345.93	↓ 4.3%	62536.16	↓ 2.5%
λ3 = -0.1↓10%	60346.62	↓ 5.8%	61831.27	↓ 3.7%	63081.37	↓ 1.6%
λ = 0.5↑50%	60991.95	↓ 4.8%	62590.36	↓ 2.4%	63939.89	↓ 0.2%
λ = 0.8↑90%	61436.45	↓ 4.2%	63119.49	↓ 1.6	64541.59	↑ 0.6%

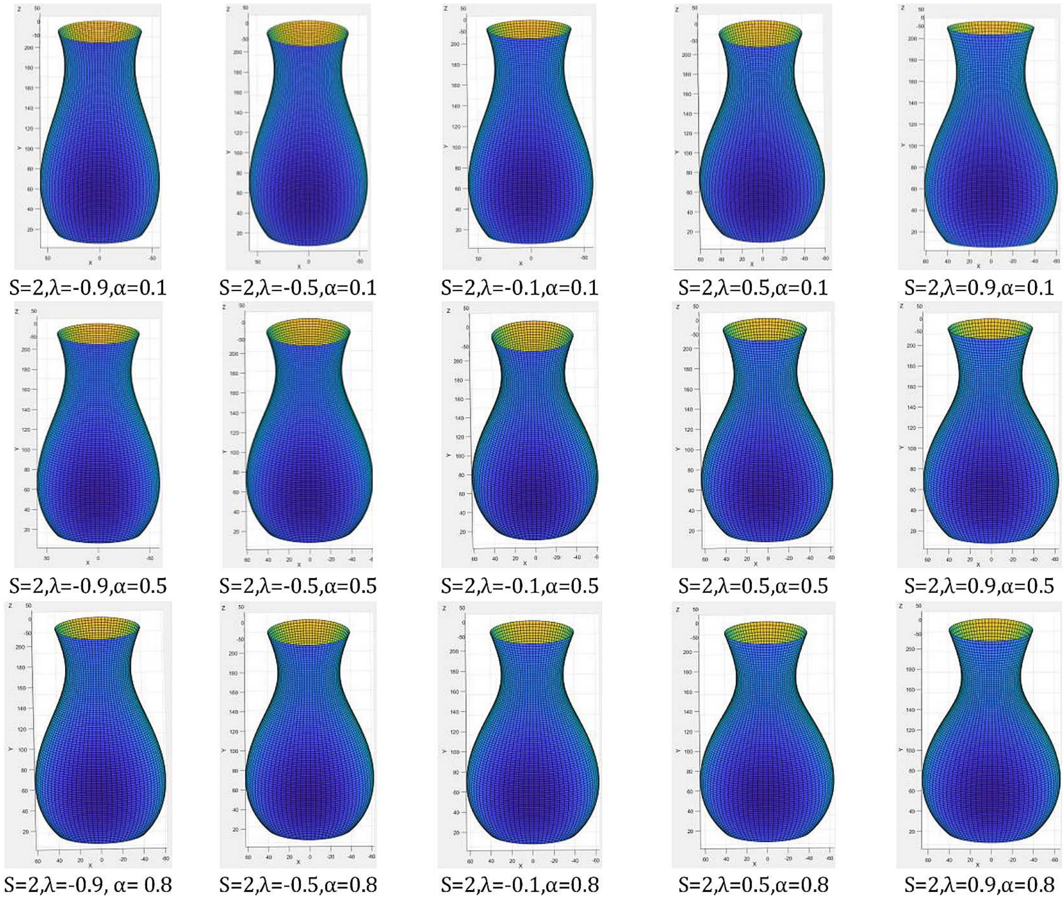

Figure 5. The revolved surfaces for the generalized Bezier curves when S =2

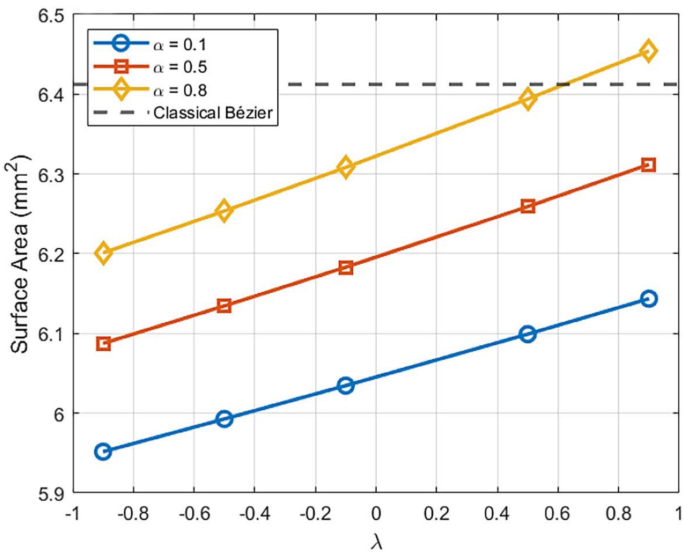

Figure 6. Plot comparison for shape parameters when s=2

values, yielding a smoother and more stable surface configuration.

Figure 10 illustrates that increasing the value of λ generally reduce the geometric response, while the parameter α controls the sensitivity of this reduction. The interaction between the shape parameters at S=4 as evidenced by the intersection behavior and varying slops of the response curve. The surface area is greater than the classical Bezier curve once λ is less than -0.4 and starts to decrease heavily; as the value of α decreases,

Table 2. Results of (25) experiments when S=3, TFC=Trend From the Classical

λ	α1 = 0.1↓90%	TFC	α2 = 0.5↓50%	TFC	α3 = 0.8↓20%	TFC
λ1 = -0.9↓90%	61791.17	↓ 3.6%	61587.25	↓ 3.9%	61607.78	↓ 3.9%
λ2 = -0.5↓50%	59505.88	↓ 7.2%	60526.07	↓ 5.6%	61708.64	↓ 3.8%
λ3 = -0.1↓10%	57306.37	↓ 10.6%	59481.33	↓ 7.2%	61880.74	↓ 3.5%
λ = 0.5↑50%	54158.75	↓ 15.5%	57946.29	↓ 9.6%	62237.34	↓ 2.9%
λ = 0.8↑90%	52158.38	↓ 18.6%	56945.8	↓ 11.2%	62550.5	↓ 2.4%

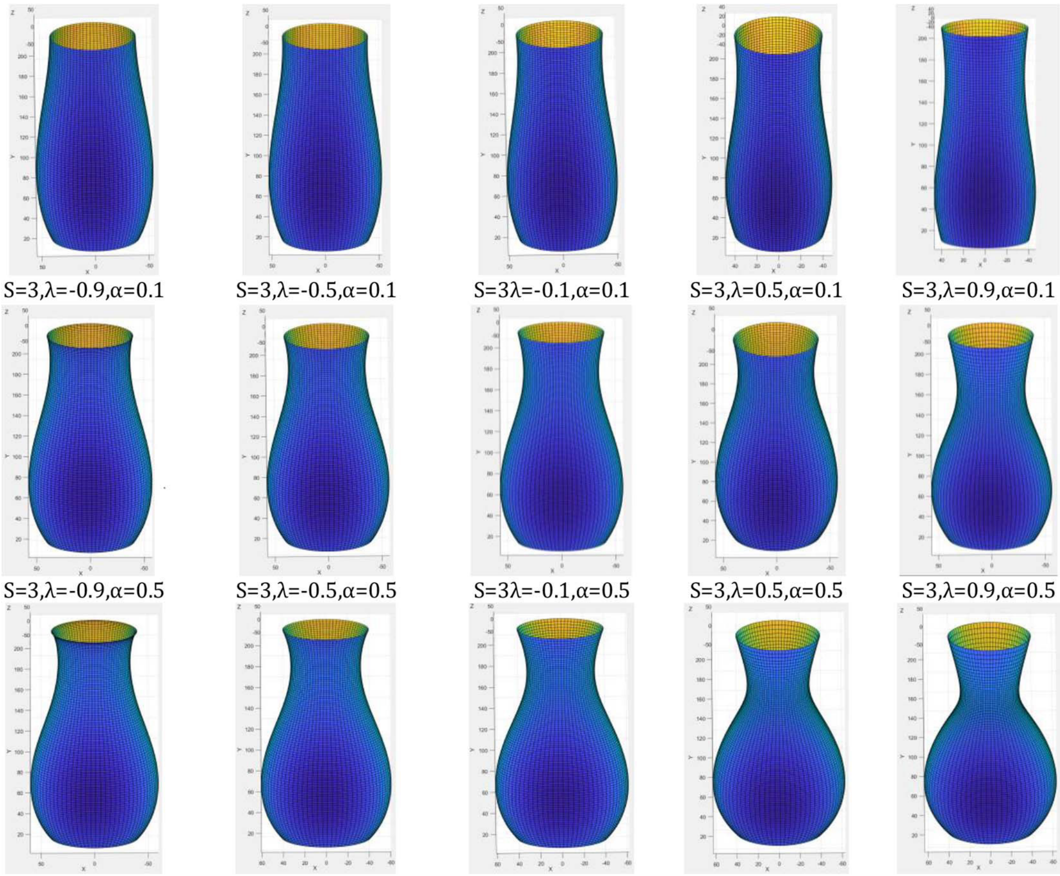

S=3,λ=-0.9,α=0.1 S=3,λ=-0.5,α=0.1 S=3λ=-0.1,α=0.1 S=3,λ=0.5,α=0.1 S=3,λ=0.9,α=0.1

S=3,λ=-0.9,α=0.5 S=3,λ=-0.5,α=0.5 S=3λ=-0.1,α=0.5 S=3,λ=0.5,α=0.5 S=3,λ=0.9,α=0.5

S=3,λ=-0.9,α=0.8 S=3,λ=-0.5,α=0.8 S=3λ=-0.1,α=0.8 S=3,λ=0.5,α=0.8 S=3,λ=0.9,α=0.8

Figure 7. The revolved surfaces for the generalized Bezier curves when s =3

the surface area of all combinations is less than the classical Bezier curve.

After studying the influence of Bezier curve and sensitivity to shape parameters, Taguchi method was employed as an efficient statistical tool for design of experiments (DOE) to identify the most effective parameter on curve configuration. The shape parameters (factors) where (λ at 5 levels, α at 5 levels and s at 3 levels), to construct L75 orthogonal array. Since the objective was to minimize (SA), the "smaller-the-better" signal-to-noise (S/N) ratio was adopted to assess the quality of each experiment using Equation 7 [30]:

$$\frac{S}{N} Ratio = -10\, Log\, 10\, (y^2) \tag{7}$$

where: y is (SA) for each experiment.

The orthogonal array header design, factor-level, and complete experimental scheme are presented in Table 4. The best combination with minimum (SA) and maximum (S/N) ratio is experiment (60) where λ = 0.9, α = 0.1 and S = 4. The mean (S/N) ratios for S, λ and α at each level are shown in Table 5.

The influence of shape parameters on the S/N ratio are depicted in Figure 11. Showing the maximum S/N ratio for each parameter.

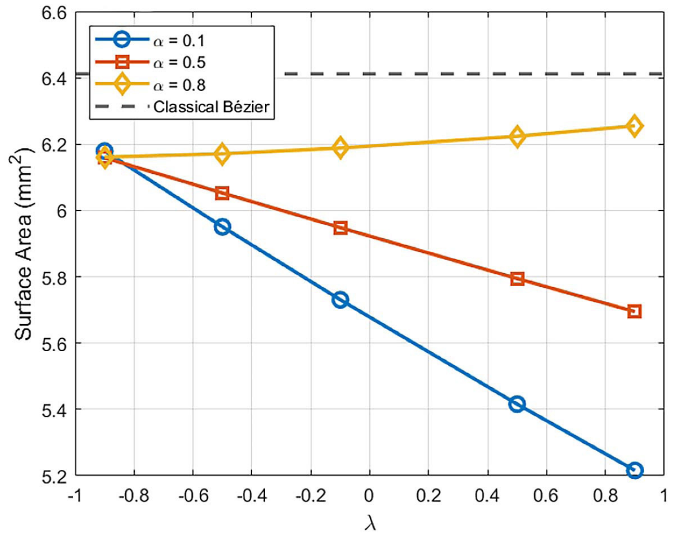

Figure 8. Plot comparison for shape parameters when s=3

Table 3. Results of (25) experiments when s=4, TFC – trend from the classical

λ	α1 = 0.1↓90%	TFC	α2 = 0.5↓50%	TFC	α3 = 0.8↓20%	TFC
λ1 = -0.9↓90%	76797.23	↑ 19.7%	69339.38	↑ 8.1%	65372.38	↑ 1.9%
λ2 = -0.5↓50%	65143.45	↑ 1.5%	63804.53	↓ 0.5%	63434.46	↓ 1.1%
λ3 = -0.1↓10%	56444.53	↓ 11.9%	58701.84	↓ 8.4%	61558.09	↓ 4%
λ = 0.5↑50%	46380.42	↓ 27.6%	51820.51	↓ 19%	58860.94	↓ 8.2%
λ = 0.8↑90%	41556.7	↓ 35.2%	47743.76	↓ 25.5%	57143.15	↓ 10.8%

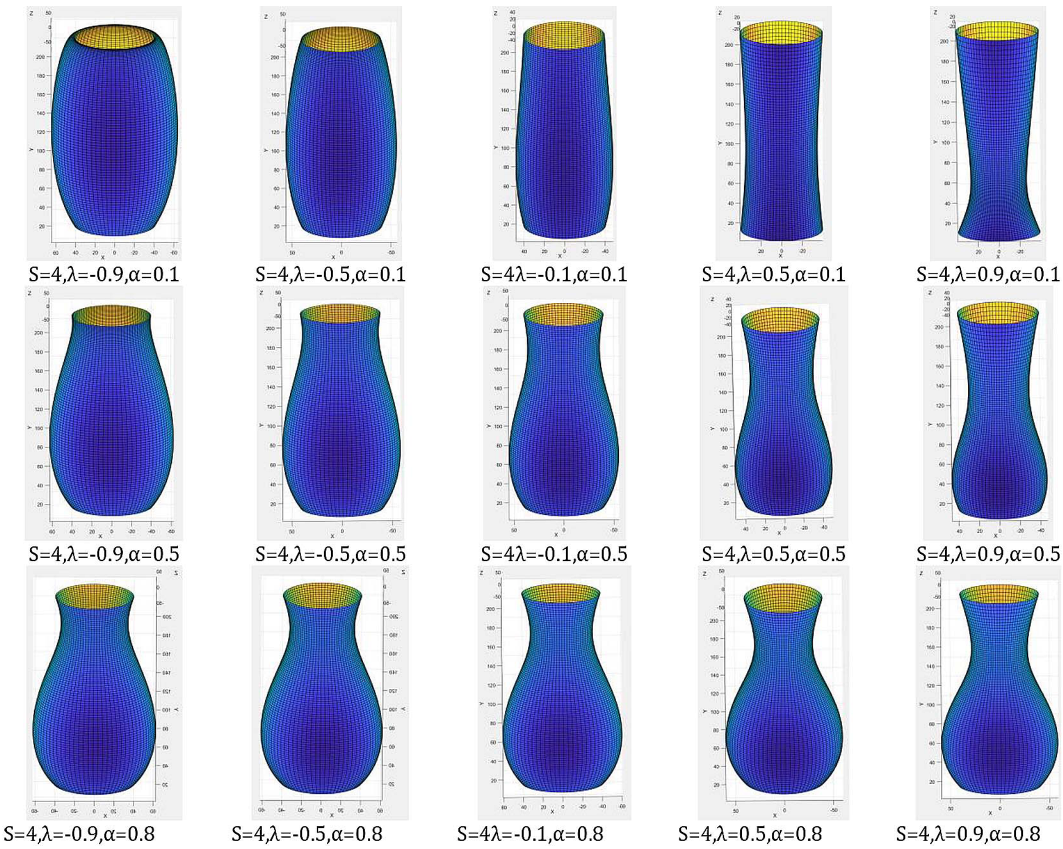

Figure 9. The revolved surfaces for the generalized Bezier curves when s =4

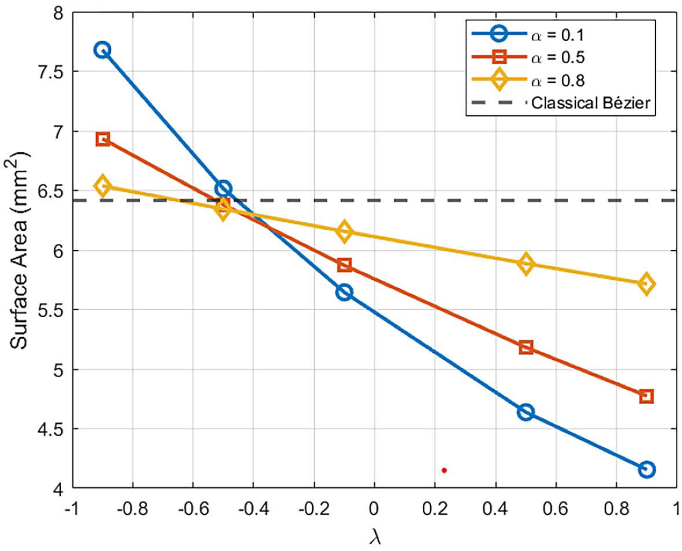

Figure 10. Plot comparison for shape parameters when s=4

Table 4. Orthogonal array and complete experiments

Ex.	S	λ	α	(SA)	S/N ratio	Ex.	S	λ	α	(SA)	S/N ratio	Ex.	S	λ	α	(SA)	S/N ratio
1	2	-0.7	0.1	59722.3	-95.5	26	3	-0.7	0.1	59722.3	-95.5	51	4	-0.7	0.1	70337.2	-96.9
2	2	-0.3	0.3	60836.2	-95.7	27	3	-0.3	0.3	60836.2	-95.7	52	4	-0.3	0.3	60716.2	-95.7
3	2	0.1	0.5	62079.9	-95.9	28	3	0.1	0.5	58965.3	-95.4	53	4	0.1	0.5	56305.9	-95.0
4	2	0.5	0.7	63475.9	-96.1	29	3	0.5	0.7	60670.6	-95.7	54	4	0.5	0.7	56240.1	-95.0
5	2	0.9	0.9	65045.4	-96.3	30	3	0.9	0.9	64807.5	-96.2	55	4	0.9	0.9	61140.1	-95.7
6	2	-0.7	0.3	60392.2	-95.6	31	3	-0.7	0.3	60793.2	-95.7	56	4	-0.7	0.3	68168.5	-96.7
7	2	-0.3	0.5	61586.7	-95.8	32	3	-0.3	0.5	60001.6	-95.6	57	4	-0.3	0.5	61200.8	-95.7
8	2	0.1	0.7	62921.3	-95.9	33	3	0.1	0.7	58965.3	-95.4	58	4	0.1	0.7	59045.4	-95.4
9	2	0.5	0.9	64417.9	-96.2	34	3	0.5	0.9	63939.1	-96.1	59	4	0.5	0.9	61751.6	-95.8
10	2	0.9	0.1	61436.5	-95.8	35	3	0.9	0.1	52158.4	-94.3	60	4	0.9	0.1	41556.7	-92.4
11	2	-0.7	0.5	61108.9	-95.7	36	3	-0.7	0.5	61054.6	-95.7	61	4	-0.7	0.5	66515.8	-96.5
12	2	-0.3	0.7	62387.2	-95.9	37	3	-0.3	0.7	61139.5	-95.7	62	4	-0.3	0.7	61989.4	-95.8
13	2	0.1	0.9	63815.7	-96.1	38	3	0.1	0.9	63171.2	-96.0	63	4	0.1	0.9	62389.8	-95.9
14	2	0.5	0.1	60991.9	-95.7	39	3	0.5	0.1	54158.8	-94.7	64	4	0.5	0.1	46380.4	-93.3
15	2	0.9	0.3	62247.1	-95.9	40	3	0.9	0.3	54169.6	-94.7	65	4	0.9	0.3	43714.4	-92.8
16	2	-0.7	0.7	61872.2	-95.8	41	3	-0.7	0.7	61421.8	-95.7	66	4	-0.7	0.7	65072.0	-96.3
17	2	-0.3	0.9	63237.5	-96.0	42	3	-0.3	0.9	62487.8	-95.9	67	4	-0.3	0.9	63053.4	-96.0
18	2	0.1	0.1	60559.2	-95.6	43	3	0.1	0.1	56237.3	-95.0	68	4	0.1	0.1	52712.3	-94.4
19	2	0.5	0.3	61762.1	-95.8	44	3	0.5	0.3	55773.4	-94.9	69	4	0.5	0.3	48523.7	-93.7
20	2	0.9	0.5	63119.5	-96.0	45	3	0.9	0.5	56945.8	-95.1	70	4	0.9	0.5	47743.8	-93.6
21	2	-0.7	0.9	62681.6	-95.9	46	3	-0.7	0.9	61894.4	-95.8	71	4	-0.7	0.9	63741.1	-96.1
22	2	-0.3	0.1	60136.4	-95.6	47	3	-0.3	0.1	58395.7	-95.3	72	4	-0.3	0.1	60572.1	-95.6
23	2	0.1	0.3	61292.4	-95.7	48	3	0.1	0.3	57411.5	-95.2	73	4	0.1	0.3	54190.2	-94.7
24	2	0.5	0.5	62590.4	-95.9	49	3	0.5	0.5	57946.3	-95.3	74	4	0.5	0.5	51820.5	-94.3
25	2	0.9	0.7	64052.6	-96.1	50	3	0.9	0.7	60488.9	-95.6	75	4	0.9	0.7	53574.8	-94.6

As the experiments show nonlinear geometric behavior, this means the effect of each parameter is not independent, but exhibits complex interaction. Thus, the analysis of variance (ANOVA) model incorporating interaction effects is adopted [31]. The ANOVA results shown in Table 6 indicate

Table 5. Main effects (λ, α, s) on S/N ratios

Effect of S		Effect of λ		Effect of α	
(S)	(S/N) Ratio	(λ)	(S/N) Ratio	(α)	(S/N) Ratio
2	-95.874	-0.7	-95.957	0.1	-94.670
3	-95.425	-0.3	-95.657	0.3	-95.041
4	-95.199	0.1	-95.267	0.5	-95.370
		0.5	-95.244	0.7	-95.700
		0.9	-95.091	0.9	-96.062

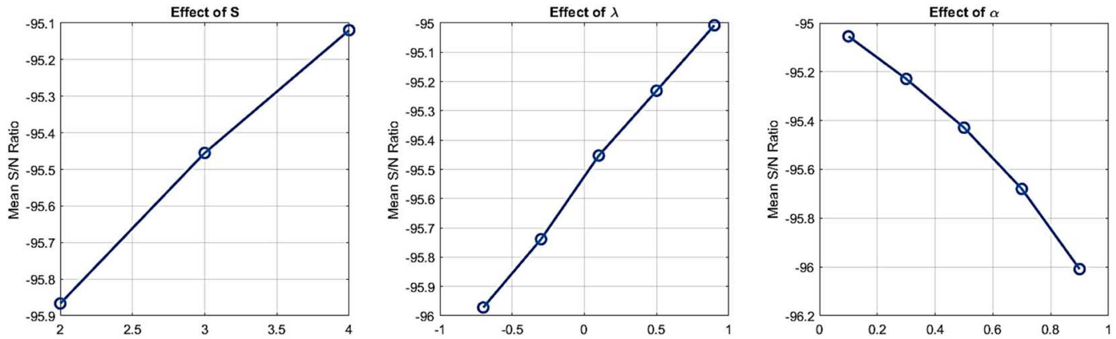

Figure 11. The influence of shape parameters on S/N ratios

Table 6. ANOVA analysis

Factors	DF	SS	Adj MS	F-value	P-value	Contribution%
S	2	2.70144e+08	1.35072e+08	31.25	0	13.6%
λ	4	3.64333e+08	9.10832e+07	21.07	0	18.4%
α	4	3.5425e+08	8.85624e+07	20.49	0	17.9 %
S & λ	8	6.18378e+08	7.72973e+07	17.88	0	31.17%
S & α	8	4.56863e+07	5.71078e+06	1.32	0.2687	2.3%
λ & α	16	1.92679e+08	1.20424e+07	2.79	0.0066	9.7%
Error	32	1.38319e+08	1.55478e+07			6.9%
total	74	1.98379e+09				

that the parameters S & λ have the maximum SS and F-value, then it is considered as the most significant influence on the SA with a contribution of 31.17%, followed by λ with 18.4%, while the parameter S and α has a smaller effect of 2.3%.

CONCLUSIONS

This study investigated the influence of shape parameters on the geometric characteristics of the generalized Bezier curve and the variations in the surface area of the generated surface of revolution. The results demonstrated the effectiveness of (λ, α, s) parameters in providing a flexible influence on geometric morphology of the generalized curve and surface without changing the control points. The extensive geometric experimentation clarified a nonlinear interaction effect between the parameters that resulted in geometries with SA greater or less than the classical Bezier curve. A statistical analysis using the Taguchi method and the S/N ratio were useful for evaluating the parameter robustness and identifying parameter settings associated with SA variability. The statistical interpretation was considered with respect to standard ANOVA assumptions and residual normality to ensure acceptable reliability of the obtained results. Taguchi and ANOVA for L75 orthogonal array demonstrated the interaction between the parameters S and λ has the maximum significant influence on SA, followed by λ. In contrast, the interaction between S and α exhibited statistically insignificant behavior (since P-value > 0.05) Indicating a comprehensively lower contribution to (SA) variation under the considered condition for the under-study experiments. However, the geometries following convex-concave transition, the non-linear interaction between shape parameters, which makes it difficult to determine where slight variations in shape parameters may produce complex geometric changes that cannot be anticipated directly.

Results show that the generalized Bezier curve gradually approaches the classical Bezier configuration when the values of shape parameters are closer to the classical parameter when λ=0, α=1, and s=1. In turn, a large deviation from these values leads to progressive losses in visual characteristics of the classical Bezier curve form and hence (SA).

Future work may extend the current analysis is by incorporating additional geometric metrics, such as maximum curvature, minimum radius of curvature, profile smoothness, and curvature continuity. These measures can better represent practical technological limitations related to manufacturability, machining constraints, stress concentration, and additive manufacturing accuracy.

REFERENCES

1. Farin, G., Hoschek, J. and Kim, M.S. Handbook of computer aided geometric design, Elsevier. 2002.
2. Ayar, A. and Sahin, B. Curves used in highway design and Bezier curves. Novi Sad J. Math, 2022; 52(1), 29–38, https://doi.org/10.30755/NSJOM.09557
3. Farin, G.E. Curves and surfaces for CAGD: a practical guide. Morgan Kaufmann. 2002.
4. Han, X.A., Ma, Y. and Huang, X. The cubic trigonometric Bezier curve with two shape parameters. Applied Mathematics Letters, 2009; 22(2), 226–231, https://doi.org/10.1016/J.AML.2008.03.015
5. Walton, D.J. and Meek, D.S. A planar cubic Bezier spiral. Journal of Computational and Applied Mathematics, 1996; 72(1), 85–100, https://doi.org/10.1016/0377-0427(95)00246-4
6. Zhu, Y., and Han, X. Curves and surfaces construction based on new basis with exponential functions. Acta Appl. Math. 2014; 129, 183–203, https://doi.org/10.1007/s10440-013-9835-2
7. Adam, J.A. What's your sphericity index? Rationalizing surface area and volume. Virginia Mathematics Teacher, 2020; 46(2), http://www.vctm.org/VOL-462
8. Gibson, I., Rosen, D., Stucker, B., and Khorasani, M. Additive manufacturing technologies. Springer, Cham, Switzerland, 2021; 17, 160–186.
9. Farouki, R.T. The Bernstein polynomial basis: A centennial retrospective. Comput. Aided Geom. Des. 2012; 29, 379–419, https://doi.org/10.1016/j.cagd.2012.03.001
10. Wen-Tao, W. and Guo-Zhao, W., Bezier curves with shape parameter. Journal of Zhejiang University-SCIENCE A, 2005; 6(6), 497–501, A0497, https://doi.org/10.1631/jzus
11. Yang, L. and Zeng, X.M. Bezier curves and surfaces with shape parameters. International Journal of Computer Mathematics, 2009; 86(7), 1253–1263, https://doi.org/10.1080/00207160701821715
12. Chen, J. Quasi-Bezier curves with shape parameters. Journal of Applied Mathematics, 2013; (1), 171392, https://doi.org/10.1155/2013/171392
13. Zhu, Y. and Han, X., Quasi-Bernstein Bezier polynomials over triangular domain with multiple shape parameters. Applied Mathematics and Computation, 2015; 250, 181–192, https://doi.org/10.1016/j.amc.2014.10.098
14. Bashir, U. and Ali, J.M. Rational cubic trigonometric Bezier curve with two shape parameters. Computational and Applied Mathematics, 2016; 35(1), 285–300, https://doi.org/10.1007/s40314-014-0194-z
15. Wu, B., Xie, J. and Li, C. A new extension of quadratic Bezier curves with multiple shape parameters. Journal of Information & Computational Science, 2014; 11(9), 3219–3227, https://doi.org/10.3963/j.issn.1671-4431.2009.20.040
16. Hu, G., Wu, J. and Qin, X. A new approach in designing of local controlled developable H-Bezier surfaces. Advances in Engineering Software, 2018; 121, 26–38, https://doi.org/10.1016/j.advengsoft.2018.03.003
17. Nazir, T., Abbas, M., Ismail, A.I.M., Majid, A.A. and Rashid, A. The numerical solution of advection–diffusion problems using new cubic trigonometric B-splines approach. Applied Mathematical Modelling, 2016; 40(7–8), 4586–4611. https://doi.org/10.1016/j.apm.2015.11.041
18. Li, H., Qin, X., Zhao, D., Chen, J. and Wang, P. An improved empirical mode decomposition method based on the cubic trigonometric B-spline interpolation algorithm. Applied Mathematics and Computation, 2018; 332, 406–419, https://doi.org/10.1016/j.amc.2018.02.039
19. Maqsood, S., Abbas, M., Miura, K.T., Majeed, A. and Iqbal, A. Geometric modelling and applications of generalized blended trigonometric Bezier curves with shape parameters. Advances in difference equations, 2020; (1), 550, https://doi.org/10.1186/s13662-020-03001-4

20. Gezer, H., Aktuğlu, H., Baytunç, E. and Atamert, M.S. Generalized blending type Bernstein operators based on the shape parameter λ. Journal of Inequalities and Applications, 2022; (1), 96, https://doi.org/10.1186/s13660-022-02832-x
21. Lu, W. and Guicang, Z. Bezier curves and surfaces with three parameters and extensions in the triangular domain. Journal of Mathematics and Informatics. 2022; 22, 29–48, http://doi.org/10.22457/jmi.v22a04204
22. Zhang, K. and Wang, H. Construction and deformation of curves and surfaces based on α-sh basis functions with shape parameters. International Journal of Applied Mathematics and Computer Science, 2025; 35(3), http://10.61822/amcs-2025-0032
23. Zhou, G. and Cai, Q.B. Approximation properties of (λ, μ)-Bernstein operators. Filomat, 2025; 39(23), 8193–8207, https://www.jstor.org/stable/27421201
24. Canlı, D. and Şenyurt, S. Bezier curves and surfaces with the generalized α-Bernstein operator. Symmetry, 2025; 17(2), 187, https://doi.org/10.3390/sym17020187
25. Kaur, J., Goyal, M. On α-Bezier curves and surfaces. Bolletino Dell'Unione Math. Ital. 2023; 16, 459–470, https://doi.org/10.1007/s40574-022-00341-9
26. Chen, X., Tan, J., Liu, Z. and Xie, J. Approximation of functions by a new family of generalized Bernstein operators. Journal of Mathematical Analysis and Applications, 2017; 450(1), 244–261, http://dx.doi.org/10.1016/j.jmaa.2016.12.075
27. Ye, Z., Long, X. and Zeng, X.M. Adjustment algorithms for Bezier curve and surface. In 2010 5th International conference on computer science & education. 2010; 1712–1716.
28. Turhan, N., Özger, F. and Mursaleen, M. Kantorovich-Stancu type (α, λ, s)-Bernstein operators and their approximation properties. Mathematical and Computer Modelling of Dynamical Systems, 2024; 30(1), 228–265, https://doi.org/10.1080/13873954.2024.2335382
29. Karakılıç, İ., Karakılıç, S., Budakçı, G. and Özger, F. Bezier curves and surfaces with the blending (α, λ, s)-Bernstein basis. Symmetry, 2025; 17(2), 219, https://doi.org/10.3390/sym17020219
30. Rashid, K.M.J. Optimize the Taguchi method, the signal-to-noise ratio, and the sensitivity. Int J Stat Appl Math, 2023; 8(6), 64–70, https://doi.org/10.22271/maths.2023.v8.i6a.1406
31. Keka, I. and Çiço, B. Comparing linear and nonlinear models for load profile data using ANOVA, AIC, and BIC. Sage Open, 2025; 15(1), https://doi.org/10.1177/21582440251326389